Ionospheric response to the interplanetary magnetic field southward turning: Fast onset and slow reconfiguration

G. Lu,[1] T. E. Holzer,[1] D. Lummerzheim,[2] J. M. Ruohoniemi,[3] P. Stauning,[4] O. Troshichev,[5] P. T. Newell,[3] M. Brittnacher,[6] and G. Parks[7]

Received 28 September 2001; revised 20 November 2001; accepted 21 November 2001; published 1 August 2002.

[1] This paper presents a case study of ionospheric response to an interplanetary magnetic field (IMF) southward turning. It is based on a comprehensive set of observations, including a global network of ground magnetometers, global auroral images, and a SuperDARN HF radar. There is a clear evidence for a two-stage ionospheric response to the IMF southward turning, namely, fast initial onset and slow final reconfiguration. The fast onset is manifested by nearly simultaneous (within 2 min) rise of ground magnetic perturbations at all local times, corroborated by a sudden change in the direction of line-of-sight velocity near local midnight and by the simultaneous equatorward shift of the auroral oval. The slow reconfiguration is characterized by the different rising rate of magnetic perturbations with latitudes: faster at high latitude than at lower latitudes. Furthermore, a cross-correlation analysis of the magnetometer data shows that the maximum magnetic perturbation is reached first near local noon, and then spread toward the nightside, corresponding to a dayside-to-nightside propagation speed of $\sim$5 km/s along the auroral oval. Global ionospheric convection patterns are derived based on ground magnetometer data along with auroral conductances inferred from the Polar UV images, using the assimilative mapping of ionospheric electrodynamics (AMIE) procedure. The AMIE patterns, especially the residual convection patterns, clearly show a globally coherent development of two-cell convection configuration following the IMF southward turning. While the foci of the convection patterns remain nearly steady, the convection flow does intensify with time and the cross-polar-cap potential drop increases. The overall changes as shown in the AMIE convection patterns therefore are fully consistent with the two-stage ionospheric response to the IMF southward turning. *INDEX TERMS:* 2463 Ionosphere: Plasma convection; 2407 Ionosphere: Auroral ionosphere (2704); 2431 Ionosphere: Ionosphere/magnetosphere interactions (2736); 2740 Magnetospheric Physics: Magnetospheric configuration and dynamics; *KEYWORDS:* ionospheric response, IMF southward turning, plasma convection, solar wind—magnetosphere—ionosphere coupling, interplanetary magnetic field changes, high-latitude changes

1. Introduction

[2] The interaction between the solar wind and the Earth's magnetosphere produces a system of plasma circulation or convection in the magnetosphere and high latitude ionosphere. The ionospheric convection configuration therefore provides important information of the solar wind-magnetosphere coupling. Although the behavior of ionospheric convection under steady interplanetary magnetic field (IMF) conditions is generally well understood, how the ionosphere responds to the changing IMF is an issue still under debate [*Ridley et al.*,1999; *Lockwood and Cowley*, 1999]. The main dispute is whether the ionospheric convection responds nearly simultaneously over the entire polar region or if the enhanced convection flows are first established in the vicinity of the dayside cusp and then propagate antisunward toward the nightside ionosphere in $\sim$15–25 min.

[3] The antisunward propagation concept was first proposed by *Lockwood et al.* [1986] based on the *F* region ion temperature changes observed by the EISCAT incoherent radar following a southward turning of the IMF. By examining the time delay between the temperature changes observed by two separate azimuthal scan beams in the afternoon sector, they estimated an eastward propagation speed of 2.6 km/s. The antisunward propagation has since been reported in several studies. Through statistical survey

[1]High Altitude Observatory, National Center for Atmospheric Research, Boulder, Colorado, USA.
[2]Geophysical Institute, University of Alaska, Fairbanks, Alaska, USA.
[3]Applied Physics Laboratory, Johns Hopkins University, Laurel, Maryland, USA.
[4]Danish Meteorological Institute, Copenhagen, Denmark.
[5]Arctic and Antarctic Research Institute, St. Petersburg, Russia.
[6]Earth and Space Sciences Department, University of Washington, Seattle, Washington, USA.
[7]Space Sciences Laboratory, University of California, Berkeley, California, USA.

0148-0227/02/2001JA000324$09.00

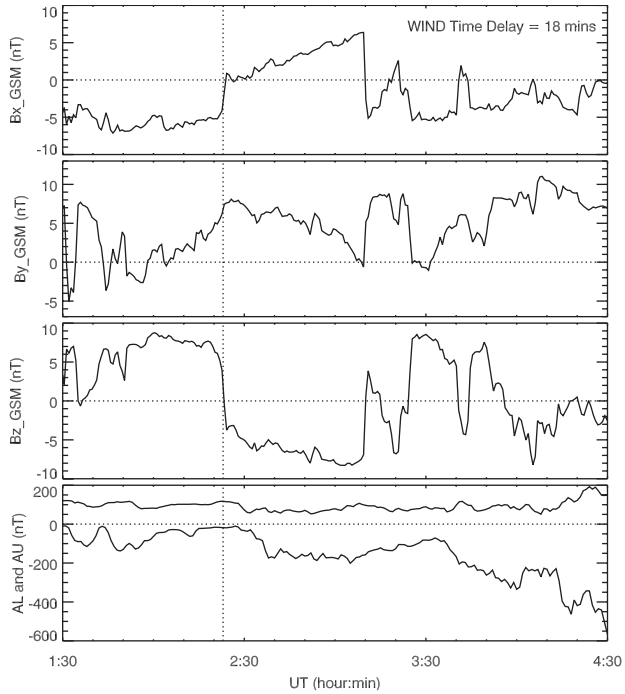

Figure 1. Variations of the interplanetary magnetic field (IMF) and the *AU* and *AL* indices from 0130 to 0430 UT on 10 January 1997. The Wind data are shown by the solid lines using the left-hand side scales, and the Geotail data are shown by the dashed lines using the right-hand side scales.

of EISCAT radar observations of plasma flow, *Etemadi et al.* [1988] and *Todd et al.* [1988] found that the response time of ionospheric convection to the IMF changes increases with distance away from local noon, corresponding to a dayside-to-nightside propagation speed of 5–10 km/s along the auroral oval. A similar time delay in ionospheric response was reported by *Saunders et al.* [1992], who examined ground magnetic perturbations over Canada in response to the north-south IMF oscillations and concluded that the response in ionospheric plasma flow spreads outward from noon toward dawn and dusk at a phase speed of ~5 km/s. This point of view was reiterated by *Khan and Cowley* [1999] using a large data set of EISCAT tristatic flow measurements. They found the epicenter of information propagation to be located at 1400 MLT and the propagation phase speed to be 6.8 km/s. A common feature of these studies is that they all were based on localized observations and had employed the cross-correlation analysis scheme.

[4] The antisunward propagation concept, however, has been seriously challenged recently by *Ridley et al.* [1997, 1998] and by *Ruohoniemi and Greenwald* [1998]. By examining the global convection patterns derived from the assimilative mapping of ionospheric electrodynamics (AMIE) procedure [*Richmond and Kamide*, 1988], Ridley et al. showed that the response of ionospheric convection flow is nearly simultaneous (within 1 min) in the entire polar region and there is no apparent propagation from dayside to nightside in the evolving convection patterns [*Ridley et al.*, 1997, 1998]. Observations from the HF radars of the SuperDARN network during a southward IMF turning event also presented a strong evidence of rapid response of line-of-sight ion drift at local time sectors extending from noon to premidnight in less than 2 min [*Ruohoniemi and Greenwald*, 1998].

[5] In this paper we present a case study using a comprehensive set of data, including a global network of ground magnetometer data, global auroral images, a HF radar, along with the aid of the AMIE procedure. We show that the different timescales regarding the ionosphere responding to IMF changes are associated with the two different aspects of the overall response, that is, the initial onset of enhanced flow and the final reconfiguration of ionospheric convection. The former is rather rapid, taking place over the entire polar ionosphere within a couple of minutes. The latter, on the other hand, is gradual, with the reconfiguration established first on the dayside and then on the nightside ~25 min later. Such a two-stage response has been recognized by some recent studies [e.g., *Jayachandran and MacDougall*, 2000; *Murr and Hughes*, 2001; *Nishitani et al.*, 2002]. We discuss the physical implications of the two-stage response.

2. Observations

[6] The three components of the IMF measured by the Wind (solid) and Geotail (dashed) satellites, respectively, from 0130 to 0430 UT on 10 January 1997, are shown in Figure 1. Wind was located upstream of the Earth at (86, −59, −4) R_E, and Geotail was in the magnetosheath at (9, −4, 1) R_E in GSE (X, Y, Z) coordinates. The close correlation between Geotail and Wind measurements yielded a time delay of 13 min for the solar wind to propagate from the Wind location to the front of the magnetopause. Notice that a time delay of 18 min for Wind would have been estimated if based on its X distance and the solar wind speed of 440 km/s [*Brittnacher et al.*, 1999]. The bottom panel of Figure 1 shows the 1-min resolution of *AU* and *AL* indices derived from the north–south component of the magnetic perturbations recorded at 69 stations located between |55°| and |76°| magnetic latitude (MLAT). The vertical dotted line marks the arrival of the IMF southward turning at the magnetopause at 0218 UT. Though there was a positive change in the IMF B_x component measured by Wind, no such change was seen by Geotail. Thus caution should be used when correlating the solar wind variations with the magnetospheric-ionospheric response, as the solar wind conditions measured upstream may not always be the same as those near the Earth. No sign change in B_y was observed by either satellite in the vicinity of 0218 UT. Prior to that, B_z was mainly northward except for a temporal southward excursion around 0135 UT. There were some fluctuations in B_y between 0130 and 0200 UT, which probably were responsible for the variations seen in the *AL* index. After the IMF turned southward *AL* gradually decreased from −20 nT to nearly −200 nT due to the enhancement of the westward electrojet on the dawnside. A substorm was developed later at 0334 UT when the first auroral brightening was observed near local midnight by the Polar satellite [*Brittnacher et al.*, 1999].

[7] Figure 2 shows a series of consecutive convection patterns in the Northern Hemisphere between 0212 and 0257 UT in 3-min increments. The patterns were derived from AMIE based on the 1-min averaged data from a global

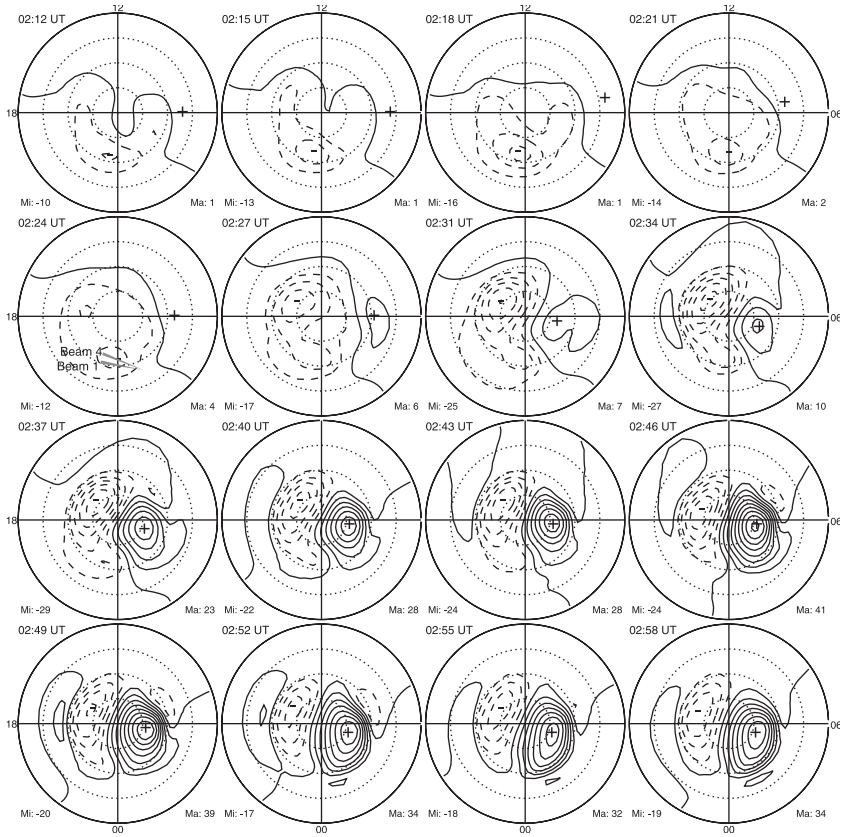

Figure 2. Consecutive convection patterns from 0212 to 0258 UT. The dashed contours represent negative potentials, and the solid contours represent positive potentials. The contour interval is 5 kV. The field of view of the beam 1 and beam 4 of the Stokkserey radar at 0225 UT is plotted over the 0224 UT convection pattern.

network of ground magnetometers (in this case there were 123 magnetometer stations worldwide, among them 87 stations were located above 50° MLAT in the Northern Hemisphere), along with auroral ionospheric conductances derived from global auroral UV images [*Lummerzheim et al.*, 1997]. In this study no data from polar-orbiting satellites (which take 20 $\sim$ 25 min to pass the polar region and $\sim$100 min to orbit the Earth) and the SuperDARN radars (which typically have a 2-min temporal resolution) were used as inputs to the AMIE fitting to avoid possible intermittent data coverage along the satellite track or in the radar's field of view. In order to eliminate the influence of the input statistical potential model on the AMIE convection patterns, particularly in regions where data coverage is poor, we have set the background potential to zero everywhere (see *Lu et al.* [2001] for more information.) From 0212 to 0224 UT the plasma convection was not well organized, consisting of mainly weak, clockwise plasma flows on the nightside half of the hemisphere. From 0227 UT and onward the convection configuration quickly evolved into a well organized two-cell pattern with antisunward convection across the polar cap.

[8] In order to see more clearly how the convection patterns evolve in association with the IMF southward turning, we show in Figure 3 the corresponding residual convection patterns. The residual patterns are obtained by subtracting a base pattern, which is the average from 0212

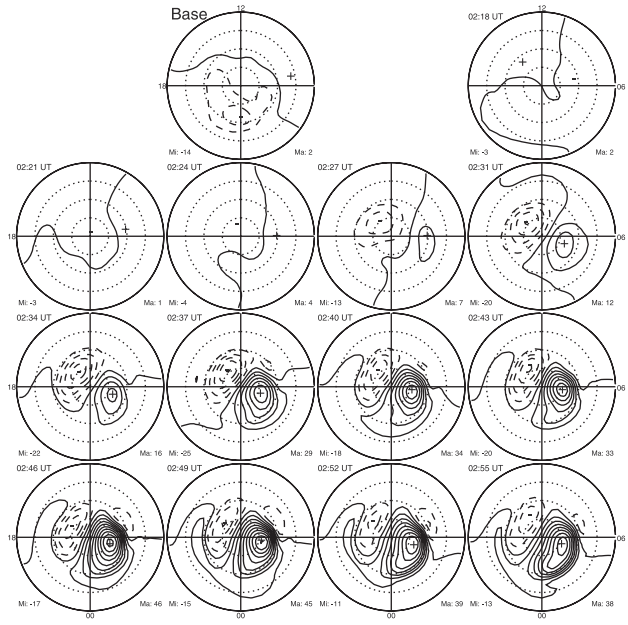

Figure 3. Residual convection patterns from 0218 to 0255 UT. The residual patterns are obtained by subtracting a steady base pattern from the corresponding patterns shown in Figure 2, where the base pattern is the average of the patterns between 0212 and 0224 UT.

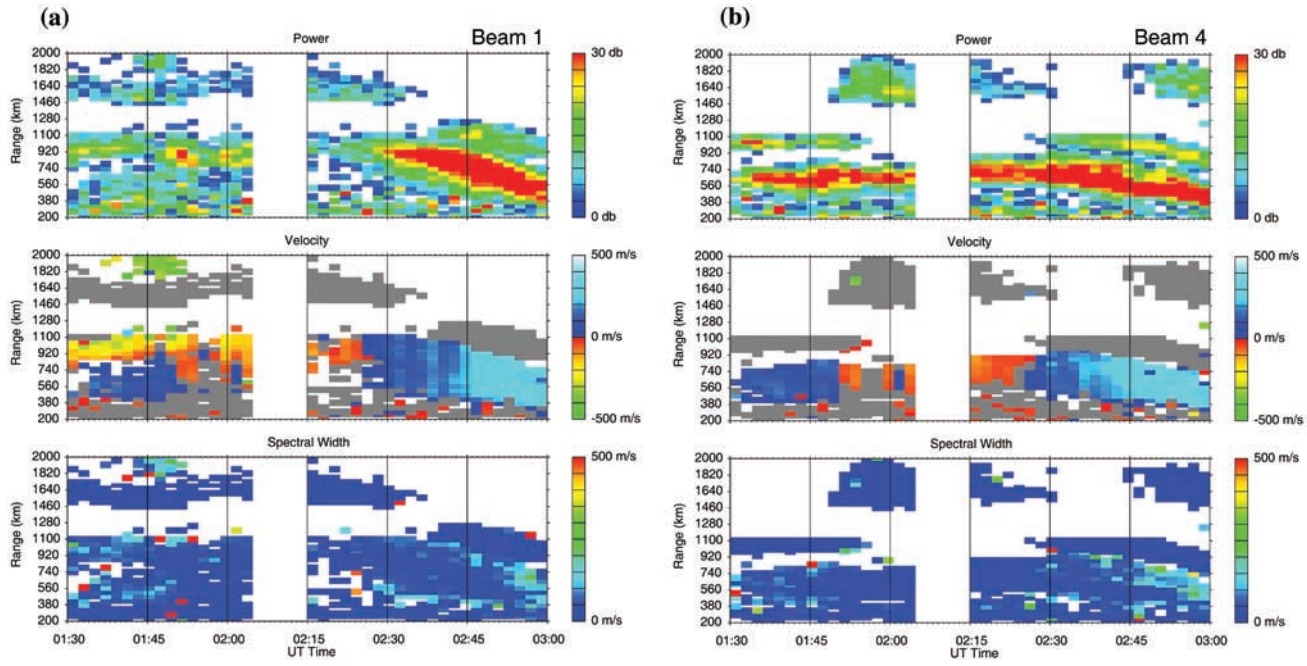

Figure 4. Plots of backscatter power, line-of-sight velocity, and spectral width from 0130 to 0300 UT by the Stokkseyri radar near local midnight. Measurements from Beam 1 are shown on the left and Beam 4 on the right. Ground scatters are indicated by the grey color.

and 0224 UT, from the overall patterns shown in Figure 2. Figure 3 demonstrates the development of the two-cell convection configuration after 0227 UT that is fully consistent with the southward IMF orientation. The potential drop of the residual convection patterns increased from 20 kV at 0227 UT to 63 kV at 0246 UT and then decreased somewhat to 52 kV at 0255 UT. While the convection flow across the polar cap intensified, the foci of the two dominant convection cells remained nearly steady throughout the interval. There was no evidence that would otherwise show the convection cells had propagated from dayside to nightside.

[9] The SuperDARN HF radars were in operation during the event. Unfortunately, most of the radars did not receive good backscatters, except for the Iceland West radar in Stokkeseyri located near local midnight. Figure 4 shows the Stokkseyri measurements of backscattered power, the line-of-sight velocity, and the spectral width from two separate beams (e.g., Beam 1 and Beam 4 whose fields of view are shown in Figure 2). Both beams observed a transition from negative velocity (away from the radar) to positive velocity (toward the radar) at ~0225 UT, which, as shown below, is consistent with the onset of magnetic perturbations at most ground magnetometer stations.

[10] The response of ground magnetic perturbations is illustrated in Figure 5 where the magnitude of horizontal magnetic perturbations at different local time sectors is plotted. The Canadian Auroral Network for the OPEN Program Unified Study (CANOPUS) magnetometer chain located near dusk (Figure 5a) shows an almost simultaneous rise of magnetic perturbations at ~0225 UT at all latitudes, except for the 2 middle stations at Rankin Inlet (RAN) and Fort Churchill (FCC) where a small bump makes the identification of the beginning of the rise somewhat difficult and the rise at these two stations may be considered at 0225 UT ± 2 min. It is also evident that the rising rate varies with latitude: faster at high latitude than at lower latitudes. The Greenland magnetometer chain located near local midnight

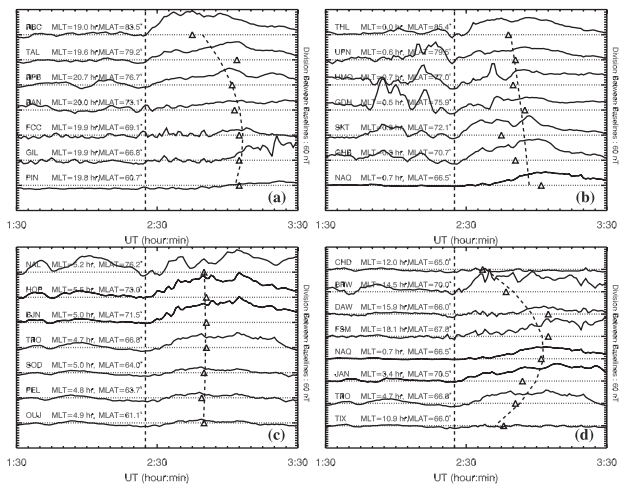

Figure 5. Stack plots of the 1-min horizontal magnetic perturbations at selected magnetometer stations: (a) CANOPUS chain, (b) Greenland chain, (c) IMAGE chain, and (d) selected stations at different MLTs between 64° and 70° magnetic latitudes. The MLT given for each station corresponds to 0230 UT. The scale is 60 nT between dividing lines for all stations except those shown as heavy solid lines (e.g., NAQ, HOP, BJN, and JAN) for which the scale is twice as indicated.

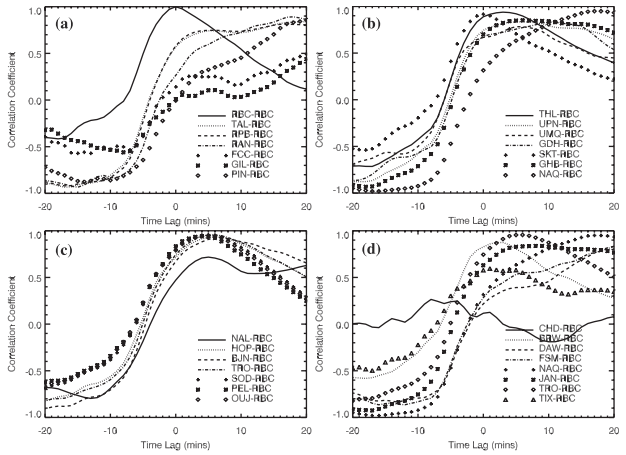

Figure 6. Distributions of the cross-correlation coefficient for the corresponding magnetometers shown in Figure 6 with respect to Resolute Bay (RBC). A positive time lag indicates RBC leading the corresponding magnetometer station.

(Figure 5b) also recorded a nearly simultaneous rise of the horizontal magnetic perturbations at all stations, so did the International Monitor for Auroral Geomagnetic Effects (IMAGE) chain near dawn (Figure 5c). Figure 5d shows the horizontal magnetic perturbations at eight selected stations located between 65° and 70° MLAT but at different MLTs. Inspection of Figure 5d shows that the six stations spanning from dusk to dawn all recorded a similar onset time in the magnetic perturbation at ~0225 UT. The two stations near local noon saw only very small increase in magnitude. By all accounts, the magnetometer data shown in Figure 5 seem to support the notion that there is a global, nearly simultaneous (within 2 min) initial response to the IMF southward turning. This is fully in agreement with previous observations of *Ridley et al.* [1997, 1998], *Ruohoniemi and Greenwald* [1998], *Lu et al.* [2001], *Murr and Hughes* [2001], and *Nishitani et al.* [2002].

[11] Cross-correlation analysis has been applied to radar and ground magnetometer data in the past [e.g., *Lockwood et al.*, 1986; *Todd et al.*, 1988; *Etemadi et al.*, 1988; *Saunders et al.*, 1992; *Khan and Cowley*, 1999]. It has helped reach the conclusion that there is a time delay in ionospheric response from dayside to nightside.

[12] We also applied the cross-correlation analysis to the magnetometer data. We chose the CANOPUS station Resolute Bay (RBC) located in the polar cap as a reference since it observed the clearest initial onset as well as the peak response. For each magnetometer station, a 40-min segment of data from 0225 to 0305 UT was used to correlate with the RBC data with a time lag of 20 min before and after the given interval. A detailed cross correlation is plotted in Figure 6. The triangles shown in Figure 5 indicate the time lags corresponding to the maximum cross-correlation coefficient at each station with respect to RBC. Here the reference time was set at when RBC reached its peak magnetic perturbation, and a positive time lag means RBC leading the corresponding station. The distribution of the triangles indicates that the cross-correlation analysis tends to relate the peak magnetic perturbation, rather than their initial onset, among the different stations. The heavy dashed curves in Figure 5 are the second-order polynomial fitting to the triangles for each magnetometer chain. For

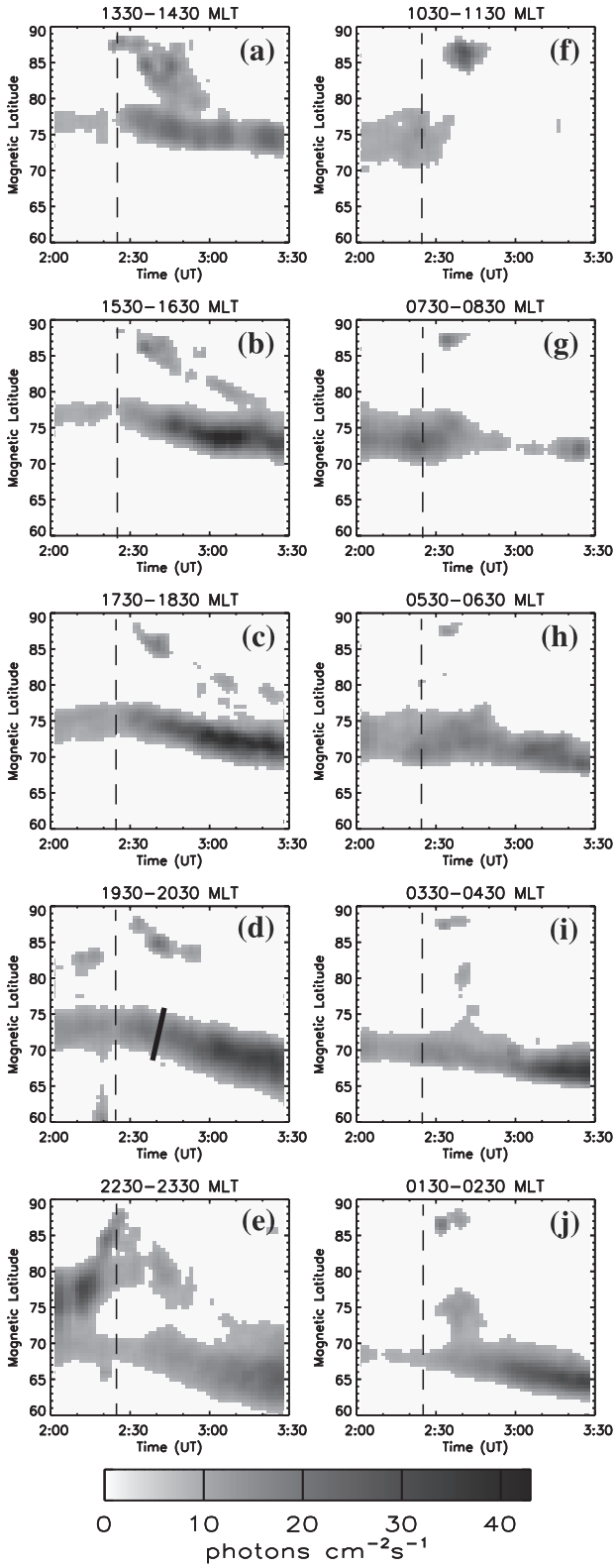

Figure 7. Keograms at different MLT sectors derived from the Polar UVI images.

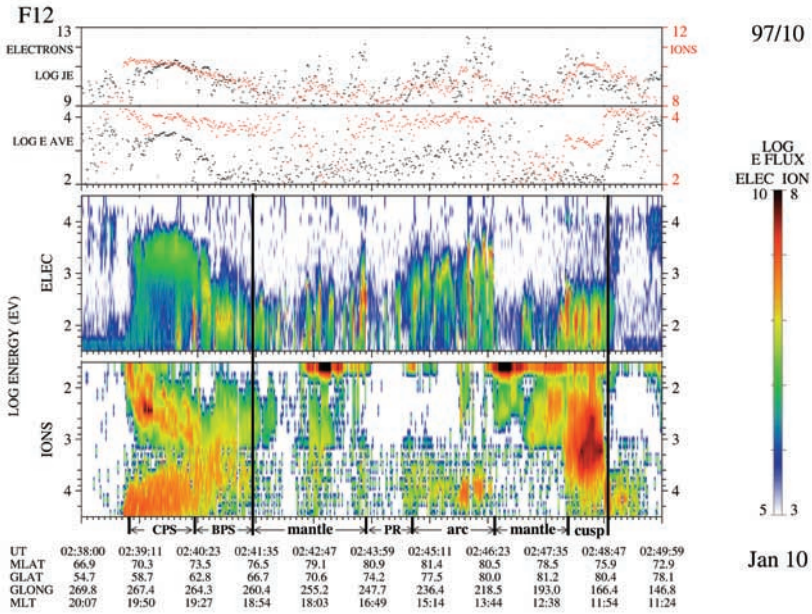

Figure 8. DMSP F12 spectrograms of differential energy flux from 0238 to 0250 UT. The different plasma regimes are identified on the bottom.

both CANOPUS and Greenland meridional chains, there was a trend that the arrival of the peak magnetic perturbations were faster at high latitudes than at lower latitudes, but the peak perturbation at the IMAGE chain was reached nearly simultaneously at all latitudes. The longitudinal chain, however, shows a more pronounced time delay in the arrival of the peak magnetic perturbation. As shown in Figure 5d, there is a time delay of ~25 min from local noon to local midnight. Considering a half circle along 67.5° MLAT (the average latitude of the longitudinal chain), this time delay would imply a dayside-to-nightside propagation speed of ~5 km/s, comparable to what has been reported previously [e.g., *Lockwood et al.*, 1986; *Todd et al.*, 1988; *Saunders et al.*, 1992; *Khan and Cowley*, 1999]. It should be remembered that all these studies have invoked the cross-correlation analysis scheme. One thing to notice is that the longest time delay was not at midnight but rather near the dusk. This may be due to the fact that the IMF B_y remained positive so that the overall convection configuration was asymmetric about the noon-midnight meridian. As illustrated in Figure 2, the direction of the polar cap convection flow was roughly along the 0900–2100 MLT meridian.

[13] Global auroral images were available during the interval of interest, allowing us to examine the motion of the entire auroral oval in response to the IMF southward turning. Figure 7 shows the keogram obtained from the Polar UVI at different MLT sectors to illustrate the changes of the auroral boundary. An auroral gap was present in the prenoon sector after ~0230 UT. The structures poleward of the main auroral oval were the remnants of a Sun-aligned arc initially formed during the previous northward IMF condition [*Brittnacher et al.*, 1999]. From postnoon to evening and into the morning sector the auroral oval, particularly the equatorward auroral oval boundary, moved systematically equatorward after ~0225 UT (marked by the vertical dashed lines). The equatorward shift of the central auroral oval, however, was not uniform, varying from a small shift (<3°) in the post noon sector as well as near dawn to a significant shift (>5°) at dusk, premidnight, and post midnight sectors. The auroral oval ceased its equatorward motion at ~0250 UT along 1330–1430 MLT, and at 0300 UT along 1530–1630 MLT, but it continued to move equatorward in the midnight sector. One important feature to note is that, while the rate of equatorward motion varied with MLT, the onset of such a shift was nearly simultaneous around 0225 UT at local times extending from postnoon to early morning, and there was no apparent time delay from dayside to nightside.

[14] While the Polar UV images showed the global distribution of the auroral oval, the DMSP F12 satellite that passed over the northern ionosphere from postdusk to prenoon provided useful additional information of the characteristics of precipitating particles. As shown in Figure 8, from 0239 to 0241 UT, the DMSP satellite crossed the auroral oval between 69.2 and 76.3 MLAT near 1930 MLT where the precipitating particles were identified as originating from the central plasma sheet (CPS) and boundary plasma sheet (BPS). The auroral oval thus identified is highlighted by the heavy bar in Figure 7d, which coincides reasonably well with the main auroral oval in the Polar UV images. Poleward of the oval was a region characterized by both low-energy (<1 keV) precipitating electrons and ions denoted as the plasma mantle [*Newell et al.*, 1991]. The poleward boundary of the oval therefore represents the open-closed boundary in the postdusk sector. Other features revealed by the DMSP spectrogram include the polar rain (PR) precipitation, the polar arcs over the dayside polar cap, and the cusp and mantle regions near local noon.

3. Discussion

[15] The response of ionospheric electrodynamic fields to IMF changes has very important implications for the

solar wind-magnetosphere-ionosphere coupling processes. Currently, there are two diametrically opposed views regarding how ionospheric convection flows are established following an IMF orientation change: simultaneous versus progressive.

[16] Studies that advocate the simultaneous ionospheric response have been based on observations taken simultaneously at various local times, such as a worldwide network of ground magnetometers [*Ridley et al.*, 1997, 1998; *Murr and Hughes*, 2001; *Nishitani et al.*, 2001] or the SuperDARN radar network [*Ruohoniemi and Greenwald*, 1998; *Shepherd et al.*, 1999]. This paper yet provides additional evidence in support of such a rapid response. Rapid ionospheric response to the IMF variations implies that the coupling process is closely controlled by the ionosphere, for example, via a fast magnetosonic wave [*Ridley et al.*, 1998]. Another possible explanation for a rapid ionospheric response to the IMF changes has been suggested by *Shepherd et al.* [1999] as due to the draping of the field lines of the new IMF state over a large portion of the dayside magnetopause. Though it is a plausible mechanism of the solar wind-magnetosphere interaction, it does not provide a full explanation for the rapid dayside-to-nightside response seen by the SuperDARN radar. The field line draping itself is a relatively slow process controlled by the magnetosheath flow velocity. In the study of *Shepherd et al.* [1999], Geotail was located near the subsolar magnetopause and IMP 8 located near the dawn flank of the magnetosheath. The IMF southward turning was observed by Geotail at 1652 UT, and by IMP 8 at 1713 UT. However, in the meantime, the global ionospheric convection changed nearly simultaneously (within 2 min) over the entire polar region at ~1703 UT. If the draping indeed was solely responsible for the ionospheric convection changes, one would expect the ionospheric change to propagate away from the dayside cusp no faster than the corresponding draping process taking place in the magnetosheath. Recently, global MHD simulations have shown that the high-latitude ionospheric convection starts to change across the entire polar cap just a few minutes after the arrival of southward IMF turning [*Lopez et al.*, 1999; *Slinker et al.*, 2001]. The fast ionospheric response, based on MHD simulations, is attributed to a fast rarefaction wave which resides inside of the magnetopause on closed field lines and channels around the Earth [*Slinker et al.*, 2001].

[17] Studies in favor of the progressive ionospheric response, on the other hand, have relied on localized observations and they all employed the cross-correlation analysis to the locally obtained data [*Lockwood et al.*, 1986; *Etemadi et al.*, 1988; *Todd et al.*, 1988; *Saunders et al.*, 1992; *Khan and Cowley*, 1999]. These studies are the observational basis for the expansion/contraction model [*Lockwood et al.*, 1990; *Cowley and Lockwood*, 1992; *Lockwood and Cowley*, 1999]. According to the model, after the IMF turns southward, magnetic reconnection creates new open field lines on the dayside. These newly opened field lines are dragged tailward by the magnetosheath plasma flow with a speed of a few hundred km/s. At the ionospheric footprints, this tailward motion corresponds to the dayside-to-nightside expansion of ionospheric convection flows of ~1 km/s across the polar cap. The propagation time from the dayside to the nightside across the polar cap corresponds to the time delay between the establishment of the subsolar magnetopause reconnection and that of the magnetotail reconnection following the southward turning of the IMF.

[18] As we have demonstrated in Figure 4, the cross-correlation analysis tends to relate the most prominent features between two data sets, such as the peaks of magnetic perturbations. While the onset of the rise in magnetic perturbation is nearly simultaneous, the rising rate varies with latitude and local time. The cross-correlation analysis is thus not suitable for detecting the initial onset, rather it tends to depict the final reconfiguration of ionospheric flows. As shown in this paper as well as in the study of *Murr and Hughes* [2001], the final reconfiguration does vary with local time: faster on dayside and slower on the nightside. Another caveat of cross-correlation analysis is that the two correlated stations may sometimes bare little overall resemblance to each other even with a reasonably high correlation coefficient. For instance, the maximum correlation coefficients for Umanaq (UMQ)-RBC and Godhavn (GDH)-RBC in Figure 6b were ~0.8, but the overall variations of UMQ and GDH in Figure 5b show very little visual similarity to that of RBC in Figure 5a.

[19] The expansion/contraction model expects the polar cap boundary to move equatorward first near the dayside cusp and subsequently on the nightside following a southward turning of the IMF [*Lockwood et al.*, 1990; *Cowley and Lockwood*, 1992; *Cowley and Lockwood*, 1992]. The motion of the polar cap boundary in association with an IMF southward turning has been reported recently by *Nishitani et al.* [2001], who found that the polar cap boundary moved equatorward first near local noon and in the premidnight sector, and then, 10~20 min later, at dusk. It should be pointed out, however, the polar cap boundary in that study was identified by using three types of totally independent observations, namely, the cusp scatter boundary observed by the Saskatoon HF radar near local noon, the equivalent current reversal boundary observed by ground magnetometers near dusk, and the poleward boundary of the plasma sheet precipitating particles measured by the DMSP satellites. It is therefore likely that the difference in response time regarding the equatorward motion of the polar cap boundary at the different local time regions may be simply due to the fact that the boundaries inferred from the different instruments are not physically identical. In this study, we identify the auroral oval based on global auroral UV images to avoid possible confusion regarding the polar cap boundary as defined by different types of observations. Global auroral images show that the initial equatorward motion of the auroral oval took place nearly simultaneously from postnoon to evening and into the morning sector, coincident with the nearly simultaneous (within 2 min) onset of horizontal magnetic perturbations over the entire polar region. But the magnitude of equatorward shift varies with MLTs, ranging from a relatively small shift (<3°) near local noon and in the morning sector to a large shift (>5°) near dusk and on the nightside. The globally coherent response of the auroral oval to the IMF southward turning shown in the Polar UV images appears to be contrary to the MHD simulations that have found a 20-min time delay for the nightside open-closed boundary to move equatorward [*Lopez et al.*, 1999; *Slinker et al.*, 2001]. We note that the poleward boundary of the main

auroral oval as depicted by the UV images may not coincide with the open-closed boundary at all MLTs. However, the in situ DMSP particle measurements show that at least in the postdusk sector the poleward boundary was indeed coincident with the open-closed boundary. Another possibility for such a discrepancy is that the open-closed boundary defined from the MHD simulations by tracing the actual field lines may not be identical to that based on the low-altitude particle characteristics.

[20] Our study has presented a clear evidence for a two-stage ionospheric response to the IMF southward turning after it arrives in the high latitude ionosphere. Such a two-stage response is a result of the complex interactions of the solar wind-magnetosphere-ionosphere system. As suggested by *Ridley et al.* [1998], the initial onset of ionospheric convection may be communicated in the form of a fast magnetosonic wave, which is about 1000 km/s in the high-latitude ionosphere. The slow reconfiguration, on the other hand, is controlled mainly by the ionosphere-magnetosphere feedback interaction. Information of the new IMF state propagates in the magnetosphere via a rarefaction wave. As shown in global MHD simulations [*Slinker et al.*, 2001], the rarefaction wave is concentrated several R_E inside of the magnetopause. It is associated with tailward flow in the noon-midnight plane and sunward flow in the equatorial plane to supply magnetic flux to the subsolar reconnection. Information about the magnetospheric state is communicated with the ionosphere via Alfvén waves along magnetic field lines. Because the ionosphere is a resistive media owing to its intrinsic coupling with the neutral atmosphere, Alfvén waves that propagate downward are partially reflected by the ionosphere, and the reflection coefficient depends on ionospheric conductivity [*Lysak*, 1990]. The combined effects of the magnetospheric communication via a rarefaction wave, the ionospheric communication via a magnetosonic wave, and most importantly, the feedback interaction between the ionosphere and the magnetosphere, determine the final equilibrium state of ionospheric convection. It is anticipated that the timescale for the final equilibrium state should be different for the different ionospheric regions since ionospheric conductivity as well as the magnetospheric magnetic field topology change from one location to another. This concept differs from the *Cowley and Lockwood* model in which the ionosphere is treated completely passive. Considering a polar cap of circular shape with a 30E diameter, which is probably reasonable or even a little conservative for a southward IMF condition, and an average anti-sunward flow speed of 1 km/s across the polar cap, the time required for the ionosphere to reconfigure would be $\sim$1 hour, not the 15–25 min as observations otherwise have shown. To overcome this apparent time discrepancy, it was suggested that the newly opened flux tubes need only to travel a few tens of R_E into the tail and the further stretching of the tube produces little subsequent change in the near-Earth system and consequently will excite little more flow [*Lockwood et al.*, 1990; *Cowley and Lockwood*, 1992].

4. Summary

[21] Using data from a satellite located at the front of the subsolar magnetopause and a worldwide network of ground magnetometers, we found the time delay between the southward turning of the IMF near the magnetopause and the initial ionospheric response to be 7 min. The onset of the initial response was nearly simultaneous at 0225 UT ($\pm$2 min) over the entire polar ionosphere. The Stokkseyri HF radar also observed a rapid change of direction of line-of-sight velocity at 0225 UT near local midnight. The AMIE convection patterns, especially the residual convection patterns, clearly show a global, coherent development of two-cell convection configuration following the IMF southward turning. The foci of convection patterns remained nearly steady, and there was no indication of any dayside to nightside propagation in the evolving convection patterns. At the same time, the convection flow continued to intensify and the cross-polar-cap potential drop increased. There was also a time delay in the maximum response of magnetic perturbations at different locations. The maximum magnetic perturbation tended to arrive at high latitudes first and then at lower latitudes, but this trend was not obvious at some local time sectors. The time delay was more pronounced for a longitudinal magnetometer chain, which clearly displayed that the peak magnetic perturbation was reached first near local noon then toward the nightside. Such a time delay is best depicted by a cross-correlation analysis. In our case the cross-correlation analysis shows a time delay of 25 min in the maximum response between local noon and local midnight, which can be translated into a dayside-to-nightside propagation speed of $\sim$5 km/s along the auroral oval. Global auroral images also show an equatorward motion of the central auroral oval after the IMF southward turning. While the onset of the equatorward shift was nearly simultaneous at all MLTs (except in the prenoon sector where aurora were absent), the magnitude of the equatorward shift did vary with MLT, with a relatively small shift near local noon and in the morning sector, and a large shift near dusk and on the nightside. Our study strongly suggests a two-stage ionospheric response to the IMF changes, consisting of the fast initial onset and the slow final reconfiguration. Such a two-stage response is a consequence of the complex interplay of several magnetospheric and ionospheric processes, including a fast rarefaction wave in the magnetosphere, a fast magnetosonic wave in the polar ionosphere, and most importantly, the feedback interaction between the ionosphere and the magnetosphere.

[22] **Acknowledgments.** We would like to express our gratitude to T. Hughes at the Canadian Space Agency, L. Hakkinen at Finnish Meteorological Institute, L. Morris at National Geophysical Data Center of NOAA, K. Yumoto and the 210 MM Magnetic Observation Group in the STEL at Nagoya University, G. van Beek of the Geological Survey of Canada, J. Posch at Augsburg College, D. Milling at University of York, C. Maclennan at Bell Laboratories of Lucent Technologies for providing the ground magnetometer data used in this study. Data from the magnetometer chains in Greenland have been prepared by O. Rasmussen from the Danish Meteorological Institute. Work at HAO was supported in part by the NASA SEC Guest Investigator and Theory programs and by the NSF Space Weather program.

[23] Janet G. Luhmann thanks both of the referees for their assistance in evaluating this paper.

References

Brittnacher, M., M. Fillingim, G. Parks, G. Germany, and J. Spann, Polar cap area and boundary motion during substorms, *J. Geophys. Res.*, *104*, 12,251–12,262, 1999.

Cowley, S. W. H., and M. Lockwood, Excitation and decay of solar wind

driven flows in the magnetosphere-ionosphere system, *Ann. Geophys.*, *10*, 103–115, 1992.

Etemadi, A., S. W. H. Cowley, M. Lockwood, B. J. I. Bromage, D. M. Willis, and H. Luhr, The dependence of high-latitude dayside ionospheric flows on the north-south component of the IMF: A high time resolution correlation analysis using EISCAT "Polar" and AMPTE UKS and IRM data, *Planet. Space Sci.*, *36*, 471–498, 1988.

Jayachandran, P. T., and J. W. MacDougall, Central polar cap convection response to short duration southward interplanetary magnetic field, *Ann. Geophys.*, *18*, 887–896, 2000.

Khan, H., and S. W. H. Cowley, Observations of the response time of high-latitude ionospheric convection to variations in the interplanetary magnetic field using EISCAT and IMP-8 data, *Ann. Geophys.*, *17*, 1306–1335, 1999.

Lockwood, M., and S. W. H. Cowley, Comment on "A statistical study of the ionospheric convection response to changing interplanetary magnetic field conditions using the assimilative mapping of ionospheric electrodynamics technique" by Ridley et al., *J. Geophys. Res.*, *104*, 4387–4391, 1999.

Lockwood, M., A. P. van Eyken, B. J. I. Bromage, D. M. Willis, and S. W. H. Cowley, Eastward propagation of a plasma convection enhancement following a southward turning of the interplanetary magnetic field, *Geophys. Res. Lett.*, *13*, 72–76, 1986.

Lockwood, M., S. W. H. Cowley, and M. P. Freemsn, The excitation of plasma convection in the high-latitude ionosphere, *J. Geophys. Res.*, *95*, 7961–7972, 1990.

Lopez, R. E., M. Wiltberger, J. G. Lyon, C. C. Goodrich, and K. Papadopoulos, MHD simulations of the response of high-latitude potential patterns and polar cap boundaries to sudden southward turnings of the interplanetary magnetic field, *Geophys. Res. Lett.*, *26*, 967–970, 1999.

Lu, G., A. D. Richmond, J. M. Ruohoniemi, R. A. Greenwald, M. Hairston, F. J. Rich, and D. S. Evans, An investigation of the influence of data and model inputs on assimilative mapping of ionospheric electrodynamics, *J. Geophys. Res.*, *106*, 417–433, 2001.

Lummerzheim, D., M. Brittnacher, D. Evans, G. A. Germany, G. K. Parks, M. H. Rees, and J. F. Spann, High time resolution study of the hemispheric power carried by energetic electrons into the ionosphere during the May 19/20, 1996 auroral activity, *Geophys. Res. Lett.*, *24*, 987–990, 1997.

Lysak, R. L., Electrodynamic coupling of the magnetosphere and ionosphere, *Space Sci. Rev.*, *52*, 33–87, 1990.

Murr, D. L., and W. J. Hughes, Reconfiguration timescales of ionospheric convection, *Geophys. Res. Lett.*, *28*, 2145–2148, 2001.

Newell, P. T., W. J. Burke, C.-I. Meng, E. R. Sanchez, and M. E. Greenspan, Identification of the plasma mantle at low altitude, *J. Geophys. Res.*, *96*, 35–45, 1991.

Nishitani N., T. Ogawa, N. Sato, H. Yamagishi, M. Pinnock, J. P. Villain, G. Sofko, and O. Troshichev, A study of the dusk convection cell's response to an IMF southward turning, *J. Geophys. Res.*, *107*(A3), 10.1029/2001JA900095, 2002.

Richmond, A. D., and Y. Kamide, Mapping electrodynamic features of the high-latitude ionosphere from localozed observations: Technique, *J. Geophys. Res.*, *93*, 5741–5759, 1988.

Ridley, A. J., G. Lu, C. R. Clauer, and V. O. Papitashvili, Ionospheric convection during nonsteady interplanetary magnetic field conditions, *J. Geophys. Res.*, *102*, 14,563–14,579, 1997.

Ridley, A. J., G. Lu, C. R. Clauer, and V. O. Papitashvili, A statistical study of the ionospheric convection response to changing interplanetary magnetic field conditions using the assimilative mapping of ionospheric electrodynamics technique, *J. Geophys. Res.*, *103*, 4023–4039, 1998.

Ridley, A. J., G. Lu, C. R. Clauer, and V. O. Papitashvili, Reply, *J. Geophys. Res*, *104*, 4393–4396, 1999.

Ruohoniemi, J. M., and R. A. Greenwald, The response of high-latitude convection to a sudden southward IMF turning, *Geophys. Res. Lett.*, *25*, 2913–2916, 1998.

Saunders, M. A., M. P. Freeman, D. J. Southwood, S. W. H. Cowley, M. Lockwood, J. C. Samson, C. J. Farrugia, and T. J. Hughes, Dayside ionospheric convection changes in response to long period IMF oscillations: Determination of the ionospheric phase velocity, *J. Geophys. Res.*, *97*, 19,373–19,380, 1992.

Shepherd, S. G., R. A. Greenwald, and J. M. Ruohoniemi, A possible explanation for rapid, large-scale ionospheric response to southward turnings of the IMF, *Geophys. Res. Lett.*, *26*, 3197–3200, 1999.

Slinker, S. P., J. A. Fedder, J. M. Ruohoniemi, and J. G. Lyon, Global MHD simulation of the magnetosphere for November 24, 1996, *J. Geophys. Res.*, *106*, 361–380, 2001.

Todd, H., S. W. H. Cowley, M. Lockwood, D. M. Willis, and H. Luhr, Response time of the high latitude dayside ionosphere to sudden changes in the north-south component of the IMF, *Planet. Space Sci.*, *36*, 1415–1428, 1988.

M. Brittnacher, Earth and Space Sciences Department, University of Washington, Seattle, WA 98195, USA.

T. E. Holzer and G. Lu, High Altitude Observatory, NCAR, Boulder, CO 80307-3000, USA. (ganglu@ncar.ucar.edu)

D. Lummerzheim, Geophysical Institute, University of Alaska, Fairbanks, AK 99775, USA.

P. T. Newell and J. M. Ruohoniemi, Applied Physics Laboratory, Johns Hopkins University, Laurel, MD 20723, USA.

G. Parks, Space Sciences Laboratory, University of California, Berkeley, CA 94720, USA.

P. Stauning, Danish Meteorological Institute, Copenhagen, Denmark.

O. Troshichev, Arctic and Antarctic Research Institute, St. Petersburg, Russia.